

Collapse of Axionic Domain Wall and Axion Emission

Michiyasu Nagasawa

Department of Physics, School of Science, The University of Tokyo, Tokyo 113, Japan

Masahiro Kawasaki

Institute for Cosmic Ray Research, The University of Tokyo, Tanashi 188, Japan

(June 1, 2021)

We examine the collapse of an axion domain wall bounded by an axionic string. It is found that the collapse proceeds quickly and axion domain walls disappear. However axions are emitted in the collapse and its energy density increases during radiation dominated era and contributes significantly to the present mass density of the universe. In particular the axion emitted from the wall can account for the dark matter in the universe for $F_a \gtrsim 10^{10}\text{GeV}$.

98.80.Cq, 14.80.Mz, 95.35.+d

I. INTRODUCTION

The axion [1–4] is the Nambu-Goldstone boson associated with the Peccei-Quinn symmetry breaking which was invented as the most natural solution to the strong CP problem [5] of QCD. The Peccei-Quinn symmetry breaking scale F_a is stringently constrained by the consideration of accelerator experiments, stellar cooling and cosmology. The allowed range of F_a/N (axion window) is between 10^{10}GeV and 10^{12}GeV , where the integer N is the color anomaly of Peccei-Quinn symmetry.

Since the Peccei-Quinn symmetry is a global U(1) symmetry, global strings (axionic strings) are produced during spontaneous symmetry breaking. At this stage the potential for the axion field is flat, i.e., the axion is massless. However the axion has a mass at QCD scale through the instanton effect. The potential is written by

$$V(A) = f_\pi^2 m_\pi^2 \left(1 - \cos \frac{NA}{F_a} \right), \quad (1)$$

where f_π is the pion decay constant and m_π is its mass. Then the mass of the axion is given by $m_a \simeq f_\pi m_\pi / F_a / N$. This potential(1) has Z_n symmetry and takes its minimum at $A = 0, (f_a/N)\pi, 2(f_a/N)\pi, \dots, 2f_a\pi$. Z_n discrete symmetry is spontaneously broken to produce two dimensional topological defects, i.e., axionic domain walls. The property of the axionic domain wall is characterized by N . Since N domain walls stretch out from each axionic string, the network of the string-wall systems is very complicated and survives long enough to dominate the universe for $N > 1$ axionic domain wall [6]. Therefore the $N > 1$ domain wall is not accepted cosmologically.

One might expect that the density of the domain wall can be diluted in the inflationary universe. However, for the dilution mechanism to work, both the reheating temperature and the expansion rate during inflation should be smaller than F_a [7], which is rather unnatural requirement for many inflation models. Therefore the domain wall problem in the axion model is serious one.

In the case of $N = 1$, the domain wall is a disk bounded by the axionic string. The wall with the string boundary is no longer stable and it might collapse by the surface tension. In fact, since, as seen later, the surface tension is stronger than the tension due to the string for the domain wall with size much greater than the width of the wall, the dynamics of the wall is controlled by the wall tension. Therefore the string that bounds the wall cannot prevent the wall from collapsing. Typically the wall has size of horizon length ($\sim t_{QCD}$) when it is formed. Therefore the time scale for collapse is about $t_{QCD} \sim 10^{-4}$ sec and the walls disappear quickly without overclosing the universe and hence the domain wall seems harmless in the case of $N = 1$ axion model. However it is expected that a number of axions are produced when the axionic walls collapse. If produced axions are non-relativistic or cold, their energy density decreases slowly ($\propto a^{-3}$ a : scale factor) compared with the radiation density ($\propto a^{-4}$). Hence the relative contribution of axions to the total density of the universe increases with a until the universe becomes matter dominated.

In this paper we study the collapse of the axionic domain wall ($N = 1$) by the numerical integration of equations of motion for the axion field and estimate the energy density of axion field after the collapse. It is found that the energy carried by the walls is converted to the axions, which gives significant contribution to the mass density of the present universe and might account for the dark matter of the universe.

The axion emission is also expected from axionic string before t_{QCD} [8] or annihilation of axionic domain walls [10]. However, since it is shown later that parallel two domain walls go through each other without annihilation, it

is unlikely that a large number of axions are produced by interaction of two domain walls. The massless axion can be produced by axionic strings and they acquire mass after the QCD phase transition, which might give significant contribution to the total density of the present universe. However there are two independent quantitative estimations by Davis [8] and by Harari and Sikivie [9] and, unfortunately, they are quite different. The contribution from axionic domain walls is expected to be at least comparable to that from axionic strings if the estimation by Harari and Sikivie is correct.

II. DYNAMICS OF DOMAIN WALL

The dynamics of the Peccei-Quinn scalar field ϕ is described by the lagrangian:

$$\begin{aligned}\mathcal{L} &= \partial^\mu \phi^* \partial_\mu \phi + \frac{\lambda}{4} [|\phi|^2 - F_a^2]^2 \\ &= \partial^\mu \phi^* \partial_\mu \phi + V_s(|\phi|)\end{aligned}\quad (2)$$

where λ is the coupling constant. As the universe cools down, Peccei-Quinn U(1) symmetry ($\phi \rightarrow e^{i\theta} \phi$) is spontaneously broken and the scalar field has vacuum expectation value $\langle |\phi| \rangle = F_a$. After global U(1) symmetry is broken, axionic strings are formed. From causality argument, about one axionic string is produced within the horizon at $T \simeq F_a$. Since the line energy density of the string is $4\pi F_a^2$, the string density ρ_{st} is about $4\pi F_a^2 t/t^3 \sim 4\pi F_a^4 (F_a/m_{pl})^2$ which is only $\sim 10^{-13} - 10^{-17}$ of total density of the universe at the formation epoch. Defining $\phi = |\phi| \exp(iA/F_a)$, the lagrangian for axion field A is derived from eq.(2) as

$$\begin{aligned}\mathcal{L}_a &= \partial^\mu A \partial_\mu A + f_\pi^2 m_\pi^2 \left(1 - \cos \frac{A}{F_a} \right), \\ &= \partial^\mu A \partial_\mu A + V_w(A)\end{aligned}\quad (3)$$

where the second term comes from QCD instanton effect which gives axion mass $m_a \simeq f_\pi m_\pi / F_a$. The potential $V_w(A)$ has a minimum at $A = 0, 2\pi F_a$ and domain walls are produced between $A = 0$ phase and $A = 2\pi F_a$ phase. More precisely, the axion mass has temperature dependence and increase as

$$m_a(T) \simeq 0.1 m_a(T=0) (\Lambda_{QCD}/T)^{3.7}, \quad (4)$$

where Λ_{QCD} is the QCD scale $\sim 200\text{MeV}$. The domain walls are produced when the axion mass becomes greater than the expansion rate of the universe, i.e., $m_a(T_1) \simeq \dot{a}(T_1)/a$. The axionic domain wall has size of about horizon length at the formation time $t_1(T_1)$ and has the axionic string on its boundary. The surface tension of the axionic domain wall is $\sigma \simeq 16m_a F_a^2$ [11]. For wall with size R , the ratio of surface energy to string energy is given by

$$\frac{\mu R}{\sigma R^2} = \frac{4\pi F_a^2}{16m_a F_a^2 R} \simeq \frac{1}{m_a R}. \quad (5)$$

Therefore the dynamics of the axionic wall with size greater than $R^* \simeq 1/(m_a) \gg t_1$ is determined by the wall tension and the string tension can be neglected.

The cosmological evolution of the wall is determined by the surface tension and interaction of walls; the former makes the wall shrink and the latter cuts the wall into small pieces. In both cases the wall finally collapses by the surface tension. After collapse the domain walls disappear and the energy that the wall had is converted into kinetic energy of axion fields. If the energy of axion fields changes like non-relativistic particles as the universe expands, the axion energy density is

$$\rho_a(t) = \rho_{wall}(t_1) \left(\frac{a(t_1)}{a(t)} \right)^3, \quad (6)$$

where $\rho_a(t)$ and ρ_{wall} are the energy density of the axion field and the axionic wall, respectively. For relativistic axion, the axion density decreases as $\sim a^{-4}$ until axion becomes non-relativistic. Then eq.(6) is changed to

$$\rho_a(t) = \rho_{wall}(t_1) \left(\frac{a(t_1)}{a(t)} \right)^3 \left(\frac{\langle E_a \rangle}{m_a} \right)^{-1}, \quad (7)$$

where $\langle E_a \rangle$ is the average energy of emitted axion at t_1 . Assuming the mean distance and the mean radius of walls are αt_1 and βt_1 , ρ_{wall} is given by

$$\rho_{wall}(t_1) = \frac{\sigma\pi(\beta t_1)^2}{(\alpha t_1)^3} = 16\pi\alpha^{-3}\beta^2 m_a F_a^2 \left(\frac{16\pi^3\mathcal{N}}{45}\right)^{1/2} \frac{T_1}{m_{pl}}, \quad (8)$$

where \mathcal{N} is the relativistic degrees of freedom at $t_1 \simeq 1\text{GeV}$. We expect that the numerical parameters α and β are $\mathcal{O}(1)$ from causality, although the precise values should be determined by the realistic simulation of cosmological formation of the wall-string system, which is beyond the scope of the present paper.

Using the entropy density of the universe $s(= 2\pi^2\mathcal{N}T^3/45)$ and its conservation ($sa^3 = \text{const.}$), the number density of the axion can be written as

$$\frac{n_a}{s} = 380\alpha^{-3}\beta^2\mathcal{N}^{-1/2} \left(\frac{F_a^2}{T_1 m_{pl}}\right) \left(\frac{\langle E_a \rangle}{m_a}\right)^{-1}. \quad (9)$$

Then the present density of the axion is

$$\rho_a = 1.06 \times 10^6 \text{cm}^{-3} \alpha^{-3} \beta^2 \mathcal{N}^{-1/2} m_a \left(\frac{F_a^2}{T_1 m_{pl}}\right) \left(\frac{\langle E_a \rangle}{m_a}\right)^{-1}. \quad (10)$$

Since $\mathcal{N} = 289/4$, $T_1 \simeq 2\text{GeV}(F_a/10\text{GeV})^{-0.18}$ and $m_a = 6.2 \times 10^{-4}\text{eV}(F_a/10^{10}\text{GeV})^{-1}$,

$$\rho_a = 3.2 \times 10^2 \text{eVcm}^{-3} \alpha^{-3} \beta^2 \left(\frac{F_a}{10^{10}\text{GeV}}\right)^{1.18} \left(\frac{\langle E_a \rangle}{m_a}\right)^{-1}. \quad (11)$$

The contribution of the axion to the density parameter Ω is given by

$$\Omega_a h^2 = 0.030 \alpha^{-3} \beta^2 \left(\frac{F_a}{10^{10}\text{GeV}}\right)^{1.18} \left(\frac{\langle E_a \rangle}{m_a}\right)^{-1}, \quad (12)$$

where h is the Hubble constant in units of 100km/sec/Mpc . Therefore the axion density is large enough to account for the dark matter in the universe unless the axion is ultra-relativistic when it is emitted. We estimate the $\langle E_a \rangle/m_a$ by numerical simulation in the next section.

III. SIMULATION OF COLLAPSE

In order to follow the motion of domain walls, we have solved the evolution equation of the axion field numerically. When a wall piece much smaller than the cosmological horizon is considered, the cosmic expansion can be ignored. Then the field equation under the Minkowski background is written as

$$\frac{\partial^2 \phi}{\partial t^2} - \nabla^2 \phi = -\frac{\partial}{\partial \phi}(V_s + V_w), \quad (13)$$

using the potentials in the equations (2) and (3). We have employed the staggered leapfrog method to solve the differential equation. The model parameters are chosen such that the width of the wall is equal to ten simulation meshes and the vacuum energy of the string is a hundred times larger than that of the wall. The variation of the numerical value in the latter condition does not alter our conclusion since only the wall tension governs the motion of walls as we have mentioned above. The boundary condition is periodic, which is useful to check the accuracy of our calculation since the total energy in the simulation box is conserved. The solution of a static infinite planar wall under $|\phi| = v$ is used in the initial configuration. When the wall lies in yz -plane, it is expressed as

$$\frac{A(x)}{F_a} = \pi + 2 \sin^{-1}(\tanh m_a x). \quad (14)$$

Thus the scale of the inverse axion mass represents the characteristic thickness of the axionic wall. The basic numerical technique is the same one in the previous paper. See the reference [13] for more details.

First we have confirmed that approaching walls that face in parallel each other pass through one another. Widrow showed this is true in the case of a toy sine-Gordon potential [12]. We have reproduced the passing phenomenon by numerical simulations using the potential (13). Fig.1 shows the result. The initial condition is set so that the relative velocity is $0.05c$, where c is light velocity and the separation between walls is 200 meshes. Notice that the size of one mesh is equal to F_a^{-1} in our simulation and we take $m_a = 0.1F_a$. As the time evolves, two walls become close and

go away without any crush. When the initial relative velocity is much larger, for example, equal to $0.5c$, the pair annihilation of walls occurs neither. Therefore it is unlikely that annihilation of domain walls occurs and produces axions during the collision process. The possibility which is described in the reference [10] should be unfavorable.

On the other hand, in the case of the encounter of a wall with a wall edge, i.e., a string cuts the wall and the process of disintegration advances [13]. Hence by repeated intercommutations, large walls are broken to small pieces. When their size becomes comparable with the thickness scale of the wall, they collapse and radiate energy as axions. In order to see how fast and effective the wall collapse is, we have performed the simulation of the evolution of a small wall piece. As a simple example we followed the time evolution of a disk wall surrounded by a circular string in the previous work [13]. The result shows that the disk wall shrinks at the velocity of light and the energy of the wall is converted to axions. We can say that the wall collapse process is so rapid that the radiation of gravitational waves is hardly expected.

In order to see the wall collapse with higher accuracy, we have performed the simulations of a strip wall. Figs.2(a)(b)(c) demonstrate the two-dimensional distribution of V_w . The first one shows the initial configuration in which there is one strip wall of infinite height and 20 meshes length. As the time evolves, the edges of the strip approach each other, that is, the wall size decreases. Thus the wall collapse proceeds also at about the light velocity and the result of the three-dimensional simulation is confirmed. In the case of Fig.2, the initial $\dot{\phi}$ is zero everywhere in the box. However, the initial motion may make the wall move periodically so that the death of wall might be avoided. We have found that this is not the case by performing the simulations with various initial motions. Even in the most extreme case where the strings attached to the wall edges go away each other with the light velocity, such a motion could do nothing more than the slight extension of the wall life time.

Finally we have estimated the $\langle E_a \rangle / m_a$ in the simulation. The time evolution of the potential energy V_w and kinetic energy of the axion field A is shown in Fig.3(a). In these simulations, the wall edges are smoothly connected to the true vacuum region which is different from the disk wall case. Since the overestimation of the field gradient is removed by this smoothing, the quantitative analysis of energy distribution is enabled. After the wall collapse there remains only axionic waves which we identify as axions and the values of the potential and kinetic energy of the axion become constant. Since the axion waves oscillate like $\sim e^{-iE_a t}$, the ratio of the kinetic energy to potential energy is equal to $\langle E_a \rangle^2 / m_a^2$. The simulation shows $\langle E_a \rangle / m_a \simeq 3$, which means that the emitted axion is mildly relativistic and becomes non-relativistic soon by cooling due to the cosmic expansion. As mentioned before we check the accuracy of our simulation by the conservation of the total energy in the simulation box. In the simulation above the total energy is conserved within accuracy of 20%.

In order to confirm the estimated value of $\langle E_a \rangle / m_a$ we have performed the simulation of higher resolution (string width = 3 meshes, wall width = 30 meshes, wall length = 60 meshes). The result (Fig.3(b)) shows $\langle E_a \rangle / m_a \simeq 3$ which is quite consistent with the result of the lower resolution run.

Our model parameters in the simulations above correspond to $m_a / F_a = 0.1$ which is much larger than the actual axion model ($m_a / F_a \sim 10^{-23}$). To check if the estimation for $\langle E_a \rangle / m_a$ depends on m_a / F_a , we have run the simulation of thicker wall (string width = 1 meshes wall width = 50 meshes, wall length = 100 meshes) in which $m_a / F_a = 0.02$. Although the conservation of the total energy becomes as bad as 50% in this case, the result indicates that the value of $\langle E_a \rangle / m_a$ is affected only slightly, which means the generality of our estimation concerning the relativity of emitted axions.

IV. CONCLUSION

In the previous section, it is found that the axionic wall collapses with time scale R/c and the mildly-relativistic axions remain after the collapse. The estimated $\langle E_a \rangle / m_a$ is about 3, which leads to the relic density of the axion given by

$$\Omega_a h^2 \simeq 0.01 \alpha^{-3} \beta^2 \left(\frac{F_a}{10^{10} \text{GeV}} \right)^{1.18} \quad (15)$$

Since α and β are expected to be $O(1)$, the contribution of the axion to the present universe is large for $F_a \gtrsim 10^{10} \text{GeV}$ (compared with the baryon density $\Omega_B h^2 \simeq 0.013$ [14]) and might account for the dark matter of the universe. However eq.(15) should be compared with the density of the coherent oscillation of axion field (cold axion) [15,16] given by

$$\Omega_a(\text{cold}) = 6.5 \times 10^{-3 \pm 0.4} \left(\frac{F_a}{10^{10} \text{GeV}} \right)^{1.18} . \quad (16)$$

Therefore the axion from the wall has comparable to or higher density than the cold axion unless $\alpha^{-3}\beta^2$ is much less than 1. In deriving (15), we assume that the domain wall collapses rapidly after its formation. As shown in the simulations this assumption is quite reasonable for walls whose size is much smaller than the horizon. However, a large wall does not shrink until its size becomes smaller than the horizon, which leads to the increase of the density of axionic domain wall and as a result the density of the axion produced by the collapse of the wall. Therefore eq.(15) may underestimate the actual axion density and the axion from axionic walls may be more important than the cold axion.

Another important source of axions is an oscillating axionic string. Let us compare our result with the axion emission from the axionic strings. The density of the axion from the strings is given by

$$\Omega_a(\text{string}) \simeq (1 - 0.01)(F_a/10^{10}\text{GeV})^{1.18}, \quad (17)$$

where uncertainty of a factor of 100 is due to two different estimations by Davis [8] and Harari and Sikivie [9]. Thus the importance of the axion from the wall depends on which estimation is correct. The difference comes from the different assumption for the energy spectrum of the emitted axion and it is hard to judge which assumption is better. In the case of the axionic domain wall the spectrum or average energy of emitted axions can be estimated by numerical simulations more easily since axions are mostly produced at the final stage of the collapsing wall whose size is much smaller than the cosmic scale.

In conclusion, the relic density of the axion produced by the collapse of axionic walls is, at least, larger than the baryon density for $F_a \gtrsim 10^{10}$ GeV and accounts for a part or all of the dark matter in the universe. The axion from the axionic domain wall is more important than the cold axion and comparable to that from strings if Harari and Sikivie's estimation is correct. To make a more precise prediction of the relic density we have to know the numeric parameter α and β , which is beyond the scope of the present work and will be studied in future work.

MN is grateful to Professor K. Sato for his continuous encouragement. This work was in part supported by the Japanese Grant in Aid for Science Research Fund of the Ministry of Education, Science and Culture (No. 3253). Numerical computations were partially performed by SUN SPARC stations at Uji Research Center, Yukawa Institute for Theoretical Physics, Kyoto University.

-
- [1] R.D. Peccei and H.R. Quinn, Phys. Rev. Lett. **38**, 1440 (1977).
 - [2] F. Wilczek, Phys. Rev. Lett. **40**, 279 (1978).
 - [3] J.E. Kim, Phys. Rev. Lett. **43**, 103 (1979); M. Shifman, A. Vainshtein and V. Zakharov, Nucl. Phys. **B166**, 493 (1980).
 - [4] M. Dine, W. Fischler and M. Srednicki, Phys. Lett. **B104**, 199 (1981).
 - [5] G. 't Hooft, Phys. Rev. Lett. **37**, 8 (1976).
 - [6] B. S. Ryden, W. H. Press and D. N. Spergel, Ap. J. **357**, 293 (1990).
 - [7] A. Linde, Phys. Lett. **B259**, 38 (1991).
 - [8] R. Davis, Phys. Lett. **B180**, 225 (1986).
 - [9] D. Harari and P. Sikivie, Phys. Lett. **B195**, 361 (1987);
C. Hagmann and P. Sikivie, Nucl. Phys. **B363**, 247 (1991)
 - [10] D.H. Lyth, Phys. Lett. **B275**, 279 (1992).
 - [11] A. Vilenkin, Phys. Rep. **121**, 263 (1985).
 - [12] L. M. Widrow, Phys. Rev. **D40**, 1002 (1989).
 - [13] M. Nagasawa, Phys. Lett. **B318**, 53 (1993).
 - [14] T.P. Walker, G. Steigman, D.N. Schramm, K.A. Olive and H-S. Kang, Astrophys. J., **376**, 51 (1991)
 - [15] J. Preskill, M. Wise and F. Wilczek, Phys. Lett. **B180**, 225 (1983);
L. Abbott and P. Sikivie, Phys. Lett. **B180**, 133 (1983);
M. Dine and W. Fischer, Phys. Lett. **B180**, 137 (1983).
 - [16] M.S. Turner, Phys. Rev. **D33**, 889 (1986).

FIG. 1. The situation that two walls pass through each other is shown. The simulation box is one-dimensional and its size is 500 meshes. The vertical axis depicts the false vacuum energy by A field, V_w which is normalized as $V_w(\pi F_a) = 0.02$. The initial separation is 200 meshes and the initial relative velocity is 0.05c. Four figures correspond to the V_w distribution at $t = 0$, $t = 1500$, $t = 3000$, and $t = 5000$ respectively.

FIG. 2. Evolution of a strip wall whose length is 20 meshes is shown. The size of the simulation box is 300^2 . Figures pick out 100^2 part of the whole plane. The value of V_w is plotted and it is normalization as $V_w(\pi F_a) = 0.02$. The first figure is the initial configuration, the second one is that at $t = 10$, and the last is drawn at $t = 20$.

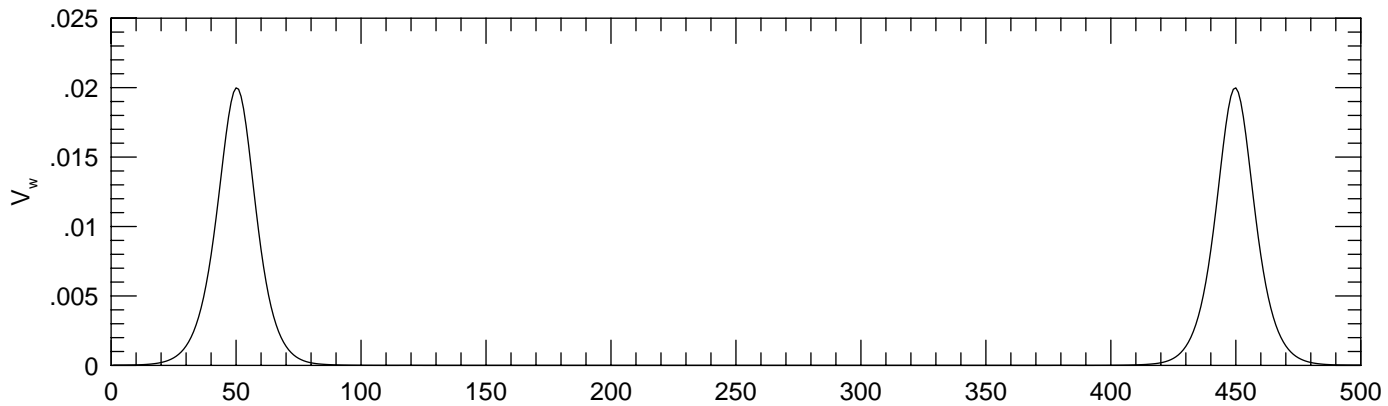
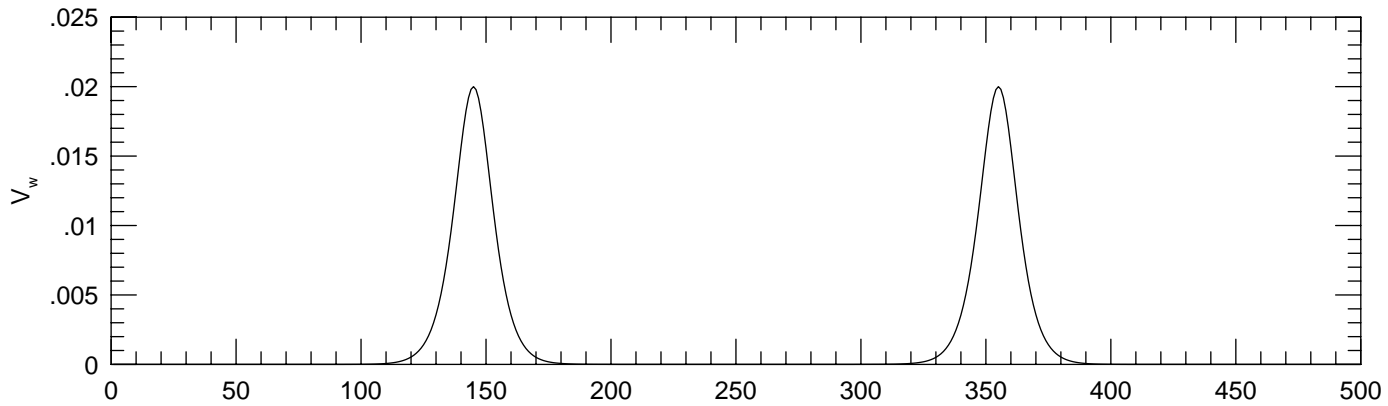
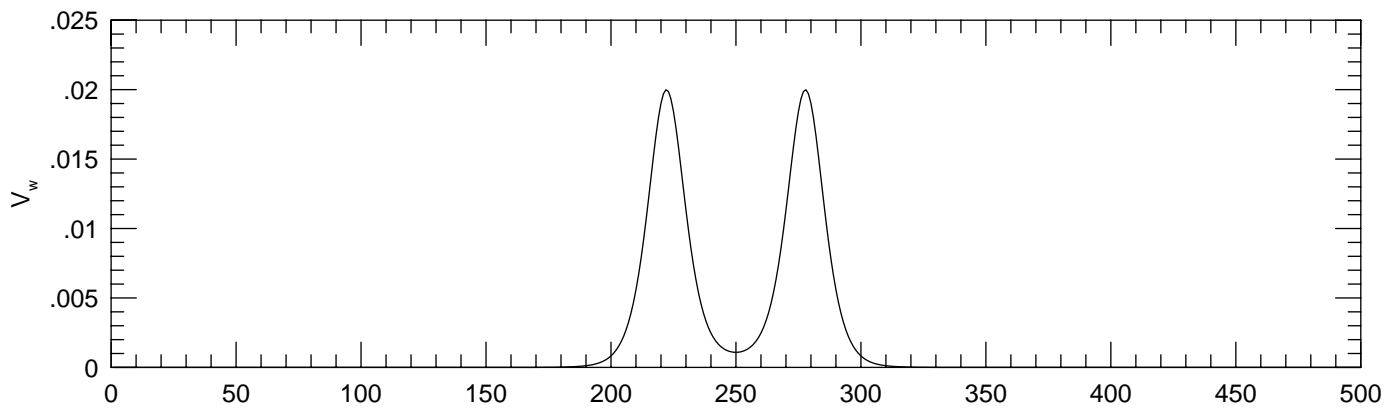
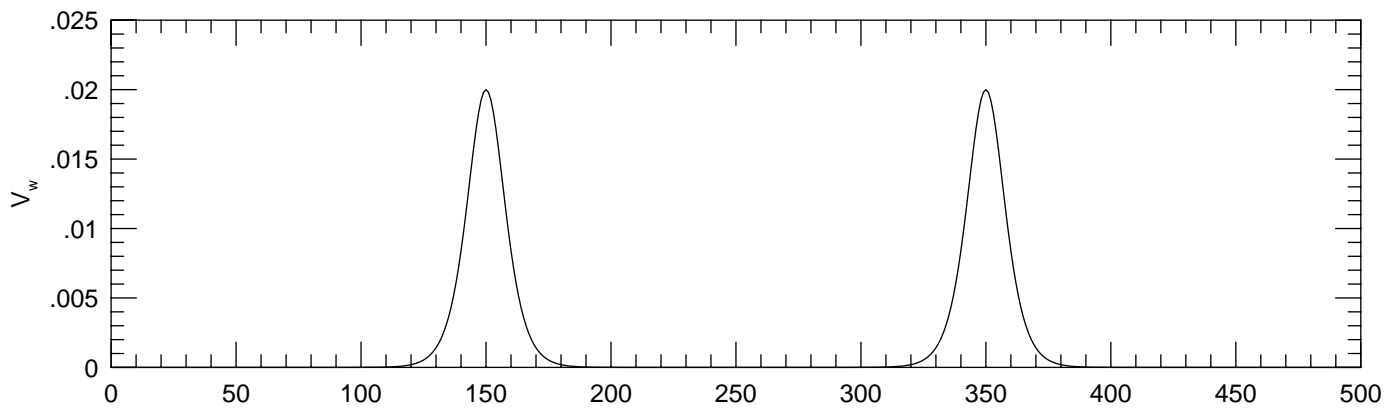
FIG. 3. Time evolution of the kinetic energy and the potential energy of the strip walls is shown. The solid lines depict the kinetic energy, $\frac{1}{2}\dot{A}^2$ and the dashed lines are the part of the potential energy by the domain wall, V_w . a) The same case as Figure (2). b) string width = 3 meshes, wall width = 30 meshes, wall length = 60 meshes.

This figure "fig1-1.png" is available in "png" format from:

<http://arxiv.org/ps/astro-ph/9402066v2>

This figure "fig2-1.png" is available in "png" format from:

<http://arxiv.org/ps/astro-ph/9402066v2>

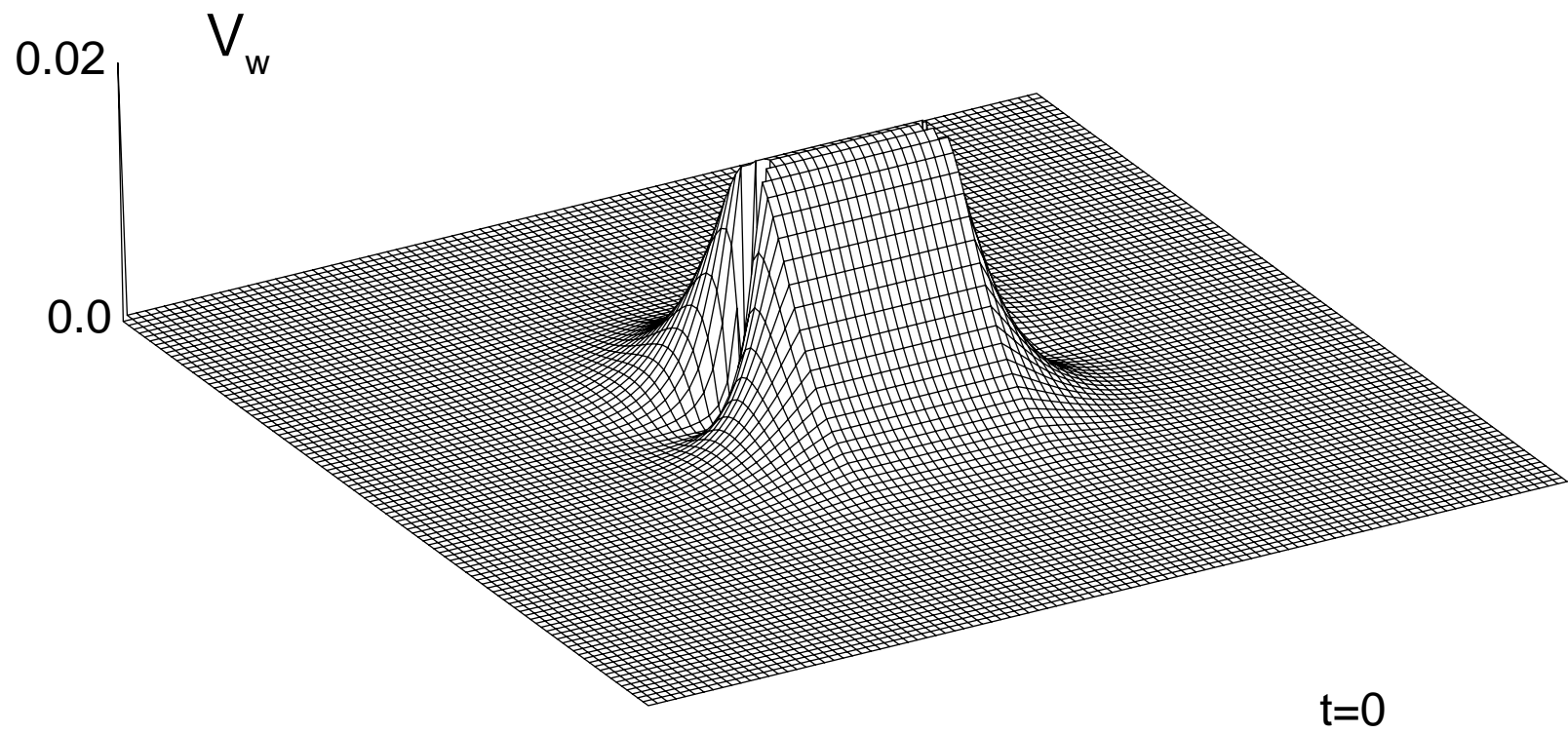


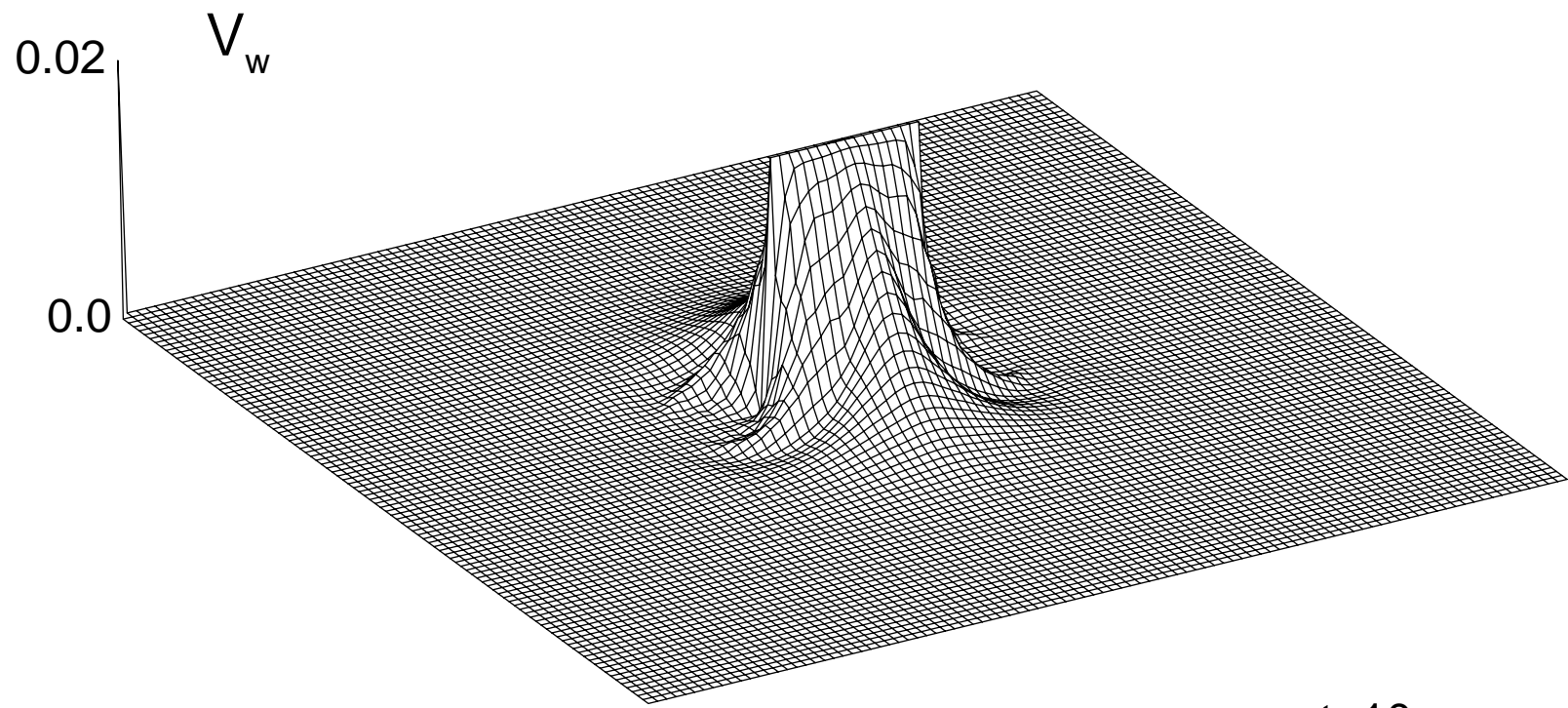
This figure "fig1-2.png" is available in "png" format from:

<http://arxiv.org/ps/astro-ph/9402066v2>

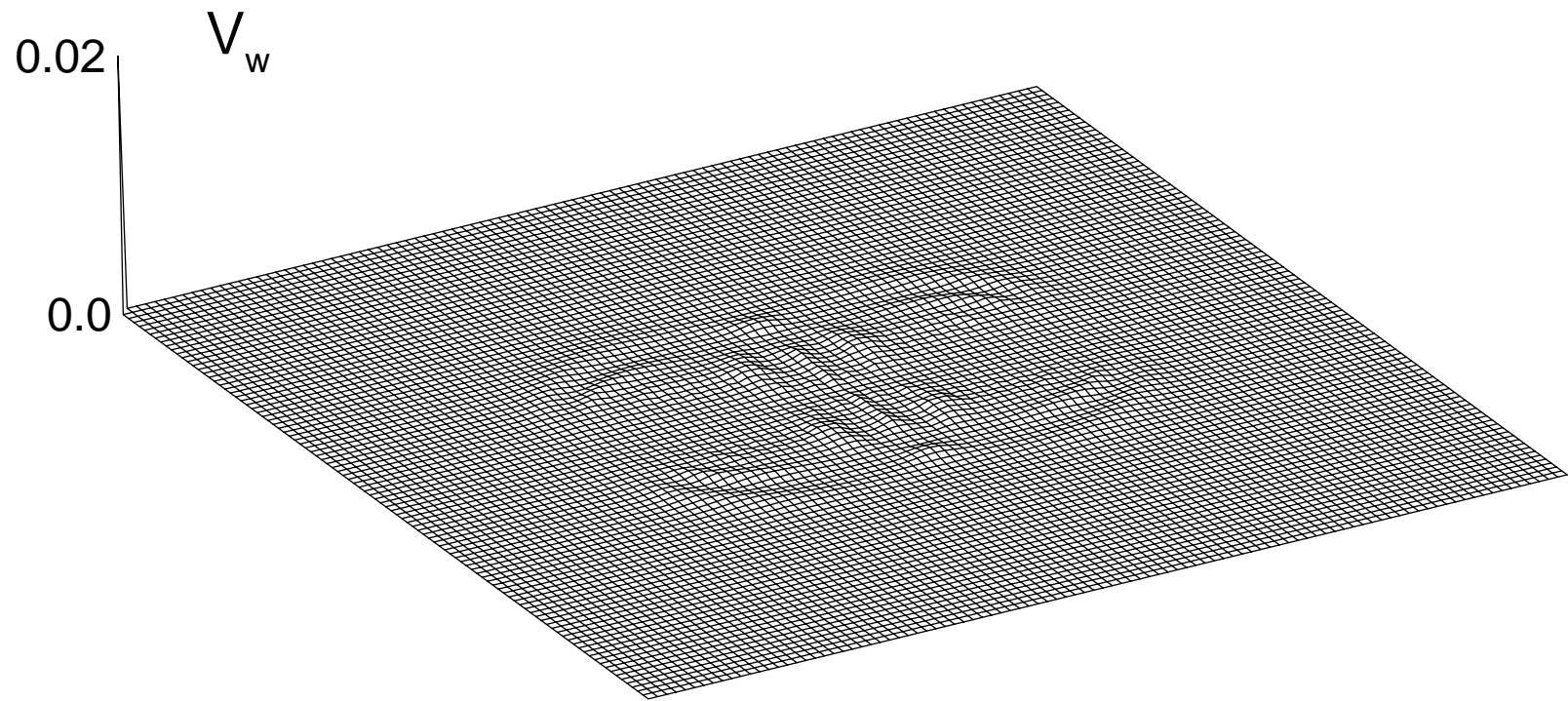
This figure "fig2-2.png" is available in "png" format from:

<http://arxiv.org/ps/astro-ph/9402066v2>





t=10



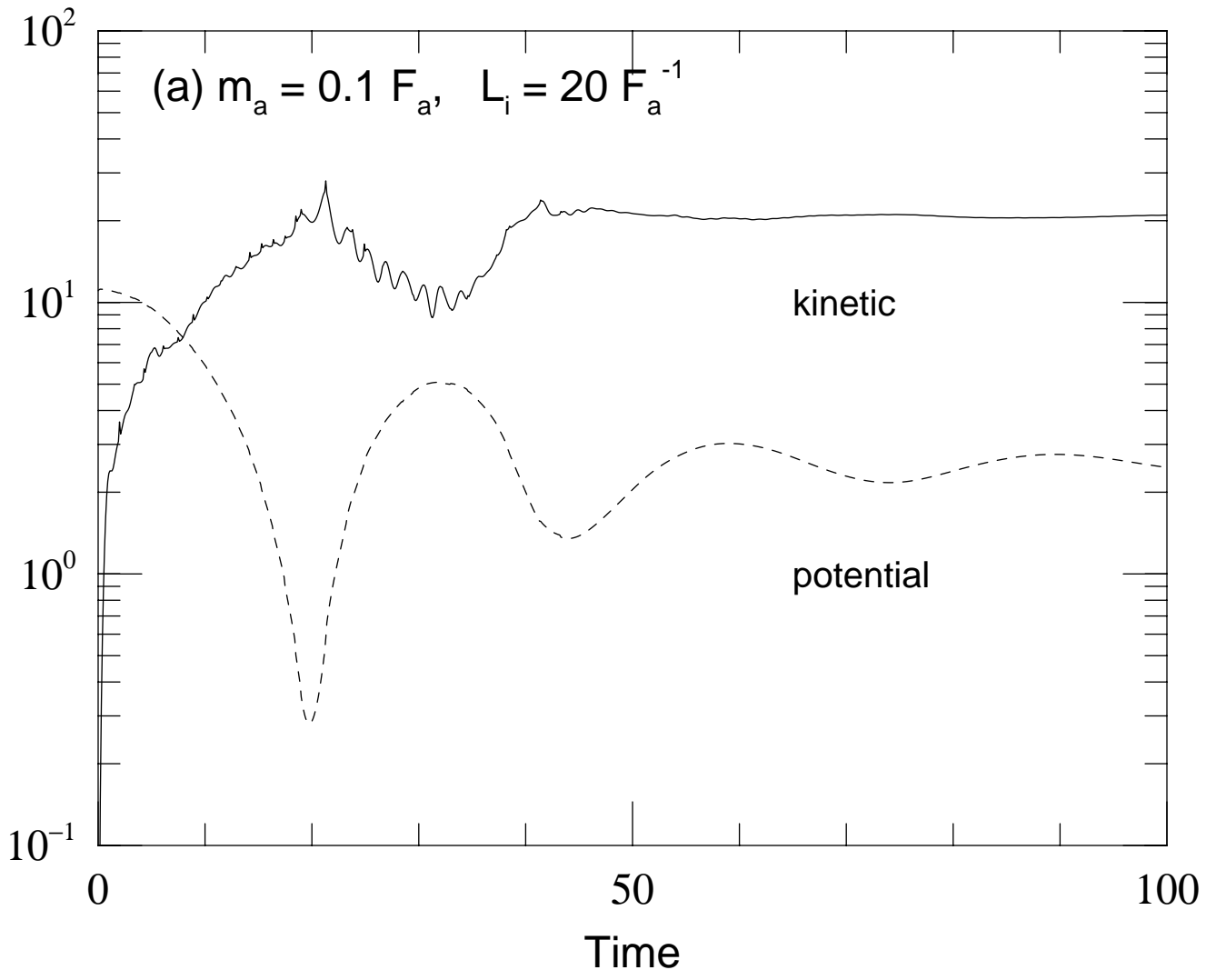
t=20

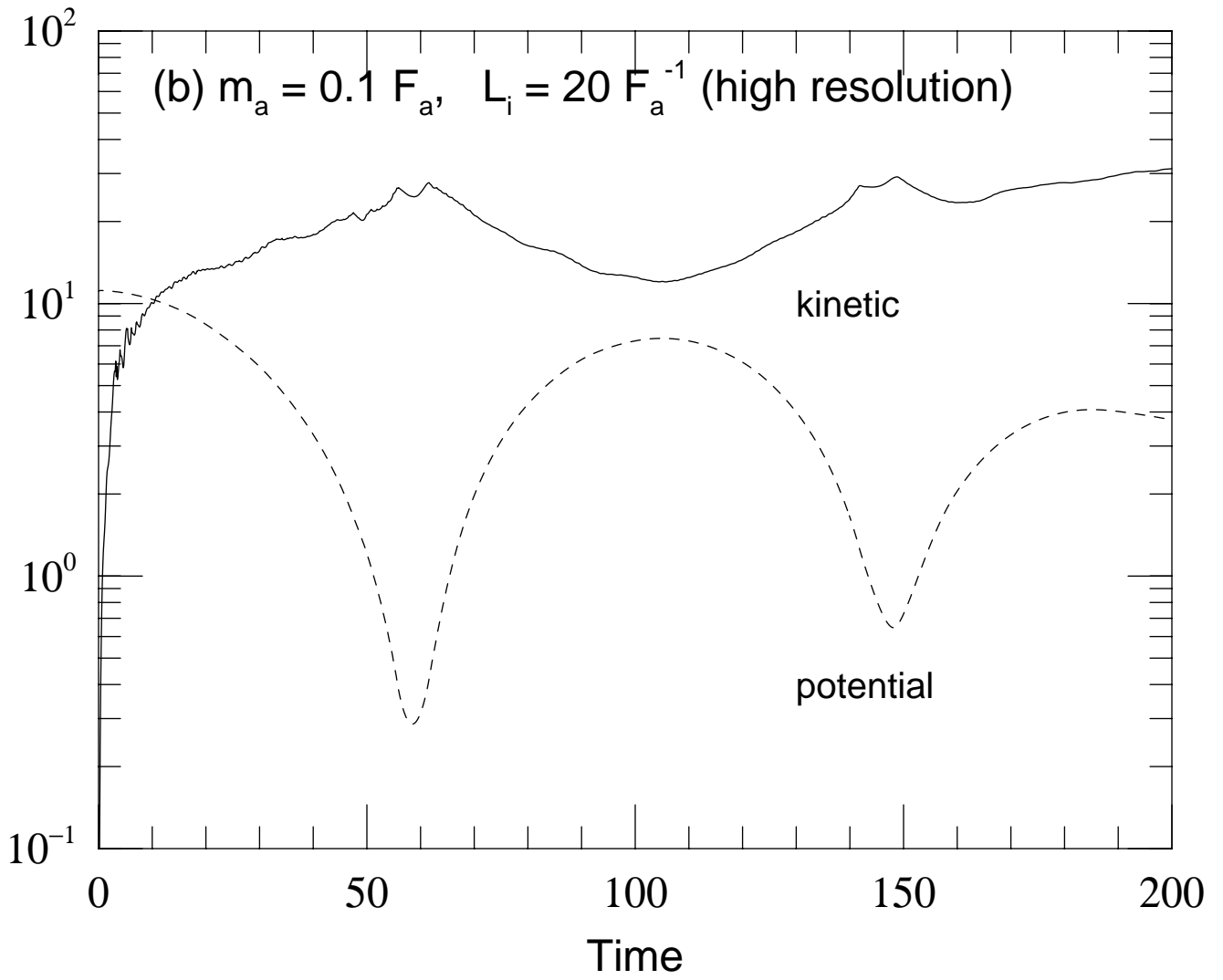
This figure "fig1-3.png" is available in "png" format from:

<http://arxiv.org/ps/astro-ph/9402066v2>

This figure "fig2-3.png" is available in "png" format from:

<http://arxiv.org/ps/astro-ph/9402066v2>





This figure "fig1-4.png" is available in "png" format from:

<http://arxiv.org/ps/astro-ph/9402066v2>